AGE (2013) 35:1143–1156
DOI 10.1007/s11357-012-9439-1

Caloric restriction-associated remodeling of rat white adipose tissue: effects on the growth hormone/insulin-like growth factor-1 axis, sterol regulatory element binding protein-1, and macrophage infiltration

Yoshikazu Chujo · Namiki Fujii · Naoyuki Okita · Tomokazu Konishi · Takumi Narita · Atsushi Yamada · Yushi Haruyama · Kosuke Tashiro · Takuya Chiba · Isao Shimokawa · Yoshikazu Higami

Received: 27 December 2011 / Accepted: 16 May 2012 / Published online: 28 May 2012

Abstract The role of the growth hormone (GH)-insulin-like growth factor (IGF)-1 axis in the lifelong caloric restriction (CR)-associated remodeling of white adipose tissue (WAT), adipocyte size, and gene expression profiles was explored in this study. We analyzed the WAT morphology of 6–7-month-old wild-type Wistar rats fed ad libitum (WdAL) or subjected to CR (WdCR), and of heterozygous transgenic dwarf rats bearing an anti-sense GH transgene fed ad libitum (TgAL) or subjected to CR (TgCR). Although less effective in TgAL, the adipocyte size was significantly reduced in WdCR compared with WdAL. This CR effect was blunted in Tg rats. We also used high-density oligonucleotide microarrays to examine the gene expression profile of WAT of WdAL, WdCR, and TgAL rats. The gene expression profile of WdCR, but not TgAL, differed greatly from that of WdAL. The gene clusters with the largest changes induced by CR but not by Tg were genes involved in lipid biosynthesis and inflammation, particularly sterol regulatory element binding proteins (SREBPs)-regulated and macrophage-related genes, respectively. Real-time reverse-transcription polymerase chain reaction analysis confirmed that the expression of *SREBP-1* and its downstream targets was upregulated, whereas the macrophage-related genes were downregulated in WdCR, but not in TgAL. In addition, CR affected the gene expression profile of Tg rats similarly to wild-type rats. Our findings suggest that CR-associated remodeling of WAT, which involves SREBP-1-mediated transcriptional activation and suppression of macrophage infiltration, is regulated in a GH–IGF-1-independent manner.

Yoshikazu Chujo, Namiki Fujii, Naoyuki Okita, and Tomokazu Konishi contributed equally to this work.

Electronic supplementary material The online version of this article (doi:10.1007/s11357-012-9439-1) contains supplementary material, which is available to authorized users.

Y. Chujo · N. Fujii · N. Okita · T. Narita · A. Yamada · Y. Haruyama · Y. Higami (✉)
Molecular Pathology and Metabolic Disease, Faculty of Pharmaceutical Sciences, Tokyo University of Science, Chiba, Japan
e-mail: higami@rs.noda.tus.ac.jp

T. Konishi
Molecular Genetics Group, Akita Prefectural University, Akita, Japan

K. Tashiro
Graduate School of Bioresource and Bioenvironmental Sciences, Molecular Gene Technics, Kyushu University, Fukuoka, Japan

T. Chiba · I. Shimokawa
Department of Investigative Pathology, Nagasaki University Graduate School of Biomedical Sciences, Nagasaki, Japan

Keywords Growth hormone · Insulin-like growth factor-1 · Caloric restriction (CR) · Lipid biosynthesis · Sterol regulatory element binding protein · DNA microarray

Introduction

Ames and Snell mutant dwarf mice, which lack growth hormone (GH), prolactin, and thyroid-stimulating hormone, live approximately 20–50 % longer than wild-type mice (Brown-Borg et al. 1996; Flurkey et al. 2001). Similarly, disrupted GH receptor/binding protein (GHR/BP) knockout (KO) mice live significantly longer than their wild-type controls (Coschigano et al. 2000). The longevity of heterozygous insulin-like growth factor (IGF)-1 receptor KO mice, and both heterozygous and homozygous insulin receptor substrate-1 KO mice (particularly females) show markedly extended lifespan compared with their counterparts (Holzenberger et al. 2003). We have also reported that heterozygous transgenic dwarf rats, bearing an anti-sense GH transgene, live longer than controls (Shimokawa et al. 2002). Based on these studies, the GH–IGF-1 axis and/or its related signaling pathways are important lifespan regulators (Bartke 2005).

Although new genetic interventions that extend the lifespan of mammals are emerging, caloric restriction (CR) remains the most robust, reproducible, and simple experimental manipulation known to extend both median and maximum lifespan, and to delay the onset of many age-associated pathophysiological changes in laboratory rodents (Weindruch and Walford 1988; Yu 1994). In general, attenuation of oxidative and other stresses, the modulation of glycemia and insulinemia, and the activation of sirtuin may be significant factors in the beneficial effects of CR (Weindruch and Walford 1988; Yu 1994; Sohal and Weindruch 1996; Masoro 2005; Sinclair 2005). Moreover, Nisoli et al. (2005) suggested that the enhanced mitochondrial biogenesis is also involved in the beneficial action of CR. Thereafter, several investigators reported that CR induces mitochondrial biogenesis (Anderson and Prolla 2009; López-Lluch et al. 2006; Shi et al., 2005). On the other hand, Hancock et al. (2011) and Gesing et al. (2011) demonstrated that CR does not increase it. Recently, we also reported that CR enhances mitochondrial biogenesis in white adipose tissue (WAT) but not in brown adipose tissue (Okita et al. 2012). Thus, the exact mechanisms underlying CR are still debated. CR animals share many characteristics with long-living dwarf mice, including smaller body size, and lower plasma insulin and IGF-1 levels (Sinclair 2005; Al-Regaiey et al. 2005). CR does not further extend the lifespan of the already long-lived GHR/BP KO mice (Bonkowski et al. 2006). In contrast, CR further extends the longevity of Ames dwarf mice and heterozygous transgenic dwarf rats bearing an anti-sense GH transgene, which live longer than their wild-type controls (Bartke et al. 2001; Shimokawa et al. 2003). Therefore, the beneficial effects of CR are not solely dependent on the GH–IGF-1 axis. In terms of the hepatic gene expression profile, CR mainly alters the expression of genes involved in the stress response, xenobiotic metabolism, and lipid metabolism. Most genes involved in stress response and xenobiotic metabolism are regulated in a GH–IGF-1-dependent manner, while those involved in lipid metabolism are regulated in a GH–IGF-1-independent manner. Moreover, CR enhances the expression of genes involved in fatty acid synthesis after feeding, and of genes encoding mitochondrial β-oxidation enzymes during food shortage, probably via transcriptional regulation by sterol regulatory element binding protein 1 (SREBP-1) and peroxisome proliferator-activated receptor (PPAR)-α, respectively (Higami et al. 2006b). Considering these findings together with serum biochemical parameters, we proposed that CR enhances lipid utilization via hepatic transcriptional changes and prevents hepatic steatosis in a GH–IGF-1-independent manner (Higami et al. 2006b).

Adipose tissue plays a central role in the regulation of both energy storage and expenditure (Saely et al. 2012). Numerous WAT-derived secretory molecules, including leptin, tumor necrosis factor (TNF)-α, and adiponectin, have been characterized, and some of these molecules play significant roles in obesity and insulin resistance (Torres-Leal et al. 2010; Ouchi et al. 2011). Therefore, WAT is now recognized as an endocrine organ rather than an inert tissue, and is implicated in the pathogenesis and complications of type 2 diabetes. It has been reported that fat-specific insulin receptor knockout mice live longer than their controls (Blüher et al. 2003). These mice show reduced adiposity and altered secretion of adipokines, including higher adiponectin and lower pro-inflammatory cytokine levels (Blüher et al. 2002). The transcription factors C/EBPα, C/EBPβ, and PPARγ are master regulators of adipocyte differentiation (Farmer 2006). Mice in which C/EBPα is replaced with C/EBPβ (β/β

mice) live longer and have reduced adiposity compared with their wild-type controls (Chiu et al. 2004). In contrast, hetero-deficient PPARγ KO mice have a shortened lifespan (Argmann et al. 2009). Transgenic mice expressing adiponectin in the liver live longer than controls, and are resistant to high-calorie diet-induced obesity (Otabe et al. 2007). Thus, altered adipose tissue gene expression and modulation of adipokine secretion seem to influence the lifespan of rodents. CR reduces adiposity and reduces adipocyte size by altering the gene expression profile (Higami et al. 2004, 2006a). CR decreases plasma insulin and leptin levels, and increases plasma adiponectin levels (Higami et al. 2005; Yamaza et al. 2007). CR also reverses age-associated insulin resistance, possibly by decreasing adiposity (Barzilai et al. 1998). Moreover, Masternak et al. (2012) reported that visceral fat removal improved insulin sensitivity, suppressed fat accumulation in the skeletal muscle, and reduced body temperature and respiratory quotient in wild-type mice and had opposite effects on long-living GHR/BP KO mice. Therefore, we hypothesized that the beneficial actions of CR may be partially mediated by WAT remodeling as well as decreasing adiposity.

In the present study, to explore the role of the GH–IGF-1 axis in CR-associated remodeling of WAT, we compared adipocyte size and gene expression profiles of WAT between CR rats and transgenic dwarf rats, bearing an anti-sense GH transgene. We propose that CR-associated remodeling of WAT, which is transcriptionally regulated by SREBP-1 and modulated by macrophage infiltration, could be regulated in a GH–IGF-1-independent manner.

Materials and Methods

Animals

The present study was conducted in accordance with the provisions of the Ethics Review Committee for Animal Experimentation at Nagasaki University. The rat characteristics and animal care are described elsewhere (Higami et al. 2006a). Briefly, in this study we used ad libitum (AL)-fed male heterozygous transgenic dwarf rats, bearing the anti-sense growth hormone transgene (tg/–; Tg), and their genetic background, Jcl:Wistar (–/–; wild-type) rats. From 6 weeks of age, both wild-type and Tg rats were divided into two groups: AL and CR (70 % of the energy intake). CR was started without adjustment for food shortage. CR rats were fed every other day. Their 2-day food allotment was equal to 140 % of the mean daily intake of AL rats. Wild-type AL (WdAL) and CR (WdCR), and Tg AL (TgAL) and CR (TgCR) rats were killed at 6–7 months of age. The day before the rats were killed, they were all provided with their allocated food 30 min before the lights were turned off in the evening and were killed after the lights were turned on the following morning. Thus, all rats were not under fasting condition when killed. Immediately after killing the rats, epididymal white adipose tissue (WAT) was collected and its weight was measured. Some of the isolated WAT was fixed in a buffered formalin solution for histological examination and the rest was immediately diced, frozen in liquid nitrogen, and stored at −80°C. Total RNA was extracted from the stored WAT for DNA microarray analysis and quantitative real-time reverse-transcription polymerase chain reaction (RT-PCR).

Histological examination

Fixed tissues were processed routinely and embedded in paraffin. Tissue sections (5 μm thick) were stained with hematoxylin–eosin. The stained sections were scanned by microscopy with a charge-coupled device camera (Nikon, Tokyo, Japan). All images were recorded after precise focusing. ImageJ 1.43u/Java1.6.0_22 software was used for all tissue analyses. The size distribution of each white area in the black-and-white images, corresponding to lipid droplets, was counted and calculated. To avoid inter-rater variation, a single observer (YC) carried out tissue analyses.

Microarrays and data normalization

Total RNA was measured using an Affymetrix Rat Genome 230_2.0 GeneChip (Affymetrix, Santa Clara, CA, USA), with four biological repeats per group. The raw data were deposited in Gene Expression Omnibus (accession code: GSE30668). The perfect match data were normalized and the expression levels of each gene were estimated using the SuperNORM data service (Skylight Biotech Inc., Akita, Japan) according to a three-parameter log-normal distribution model (Konishi et al. 2008). To reduce noise effects, the analyses were focused on genes identified as positive by two-way analysis of variance (ANOVA), with a two-sided threshold of 0.001. Out of 31,099 genes on each chip, 6,641 were positive.

Principal component analysis

To compare the effects of CR (WdAL vs. WdCR) with those of Tg (WdAL vs. TgAL), we performed principal component (PC) analysis (Jackson 2005) on the ANOVA-positive genes. To reduce the effects of individual differences between samples, the axes of the PC analysis were estimated on a matrix of each group's sample means and applied to all data, which were centered using the sample means of WdAL rats (the R scripts used are available in the Supplemental Materials and Methods). The methodology rotated the original data matrix around the center of the WdAL rats, to fit perpendicular axes toward which most of the variations in the data appeared. The distribution of each PC value was checked on a normal QQ plot and outlier genes that departed from the normality (PC1: >0.16 and < –016 in Supplemental Fig. 1; PC2: >0.1 and < –0.1 in Supplemental Fig. 2) were selected.

Evaluation of frequently occurring biological functions in gene annotations

To test the significance among categories of biological functions that appeared in the selected genes' annotations, we applied binomial statistical tests based on the frequencies found in the Gene Ontology (GO) Biological Process annotations (release 31) provided by Affymetrix (Konishi et al. 2008).

Quantitative real-time RT-PCR

To obtain cDNA, 1 μg of RNA extracted from WAT of WdAL, WdCR, TgAL, and TgCR rats was reverse transcribed using PrimeScript Reverse Transcriptase (Takara, Shiga, Japan) with random hexamers (Takara). Quantitative real-time PCR was performed using an Applied Biosystems 7300 real-time PCR system (Applied Biosystems, Carlsbad, CA, USA) with SYBR Premix ExTaqII (Takara). The primer sequences for *SREBP-1a*, *SREBP-1c*, *SREBP-2*, *fatty acid synthase* (*FASN*), *acetyl-CoA carboxylase 1* (*ACC1*), *squalene epoxidase* (*Sqle*), *mevalonate kinase* (*Mvk*), *F4/80*, *monocyte chemotactic protein-1* (*MCP-1*), *CD11c* (also known as *integrin alpha X*), *CD163*, and *TATA box binding protein* (*TBP*) are shown in Table 1. TBP was used as a normalization control. The amount of target mRNA relative to *TBP* mRNA in the three groups was obtained. Data from three to six rats per group are expressed as means±SEM and were compared using Tukey's *t* test. Differences were considered statistically significant at $P<0.05$.

Results

CR markedly reduced the body weight of both wild-type and Tg rats. Tg also significantly decreased the body weight of both AL and CR rats (WdAL, 486.9±29.9 g; WdCR, 349.7±15.6 g; TgAL, 310.3±12.1 g; TgCR, 237.8±25.7 g). Similarly, CR markedly reduced the epididymal WAT weight of both wild-type and Tg rats. Tg also significantly reduced it in both AL and CR rats (WdAL, 7.02±1.04 g; WdCR, 4.96±0.97 g; TgAL, 4.76±0.74 g; TgCR, 4.32±0.88 g). In contrast, WAT weight as a percentage of body weight, which represents adiposity, did not differ among WdAL, WdCR, and TgAL rats, but it was markedly increased in TgCR rats (WdAL, 1.44±0.18 %; WdCR, 1.42±0.27 %; TgAL, 1.53±0.22 %; TgCR, 1.81±0.26 %).

CR significantly reduced the size of white adipocytes, but this effect was predominantly found in wild-type rats compared with Tg rats (Fig. 1a–d). Tg also slightly reduced their size, but it was likely that the effect of Tg was less than that of CR (Fig. 1a and c). In fact, the median adipocyte size was significantly smaller in WdCR than in WdAL, but not in TgCR compared with TgAL. It was slightly but significantly smaller in TgAL than in WdAL (WdAL vs. WdCR: $p=0.001$, TgAL vs. TgCR: $p=0.100$, WdAL vs. TgAL: $p=0.026$, Fig. 1f). The percentage of adipocytes showing >5,000 μm^2 was also significantly lower in WdCR than WdAL, but not in TgCR compared with TgAL. It was slightly but significantly smaller in TgAL than in WdAL (WdAL vs. WdCR: $p<0.001$, TgAL vs. TgCR: $p=0.090$, WdAL vs. TgAL: $p=0.039$, Fig. 1g). In WAT of WdCR and TgCR, the adipocytes were predominantly 1,000–3,000 μm^2 in area, whereas those in WdAL and TgAL WAT showed a much greater size distribution. This pattern was more significant in WdAL than in TgAL rats (Fig. 1e).

Based on the DNA microarray data of WdAL, WdCR, and TgAL, using high-density oligonucleotide microarrays, 6,641 genes were positive based on two-way ANOVA ($P<0.001$). These genes were applied to PC analysis. The PC scores for each group and their

Table 1 List of primers for real-time RT-PCR

	Forward	Reverse
SREBP-1a[a]	5′-CCGAGGTGTGCGAAATGG-3′	5′-TTGATGAGCTGAAGCATGTCTTC-3′
SREBP-1c[b]	5′-GGAGCCATGGATTGCACATT-3′	5′-GGCCCGGGAAGTCACTGT-3′
SREBP-2	5′-CGATCAAGTCAGCAGCCAAG-3′	5′-AATCCCACAGAGTCCACAAAAG-3′
FASN	5′-AGCAGGCACACACAATGGAC-3′	5′-GAAGAAGAAAGAGAGCCGGTTG-3′
ACC1	5′-TGGATGAACCATCTCCGTTG-3′	5′-CATGTGAAAGGCCAAACC-3′
Sqle	5′-GTCTCCGGAAAGCAGCTATGG-3′	5′-CTCCTTGGTGTCCCCAGTCTC-3′
Mvk	5′-CAGAGCAATGGGAAAGTGAGC-3′	5′-TCTCCAGTTGCTCCAAGGTG-3′
MCP-1	5′-CCAGCCAACTCTCACTGAAGC-3′	5′-CTTCTTTGGGACACCTGCTG-3′
F4/80	5′-GGCCAAGATTCTCTTCCTCAC-3′	5′-TCACCACCTTCAGGTTTCTCAC-3′
CD11c	5′-AGCACACGGGGAAGGTTGTC-3′	5′-CAGGTCAGTGCTGCCATCTCTATC-3′
CD163	5′-ACAAATACGTGGCTCTTTCCTG-3′	5′-ATGGGATTTCTCCTCCAACC-3′
TBP	5′-CAGTACAGCAATCAACATCTCAGC-3′	5′-CAAGTTTACAGCCAAGATTCACG-3′

[a] Koo et al. (2009)

[b] Yang et al. (2001)

gene expressions are shown in a scatter plot (Fig. 2a). The PC1 and PC2 axes almost coincided with the effects of CR (WdAL vs. WdCR) and Tg (WdAL vs. TgAL), respectively. CR was more effective than Tg because the gene expression plots were more widely distributed along the PC1 axis than the PC2 axis. Indeed, 199 and 226 genes showing PC1 >0.16 and PC1 < –0.16 were upregulated and downregulated by CR, respectively. In contrast, only 65 and 118 genes showing PC2 >0.1 and PC2 < –0.1 were upregulated and downregulated by Tg, respectively (Table 2). Binomial tests were performed using the selected genes

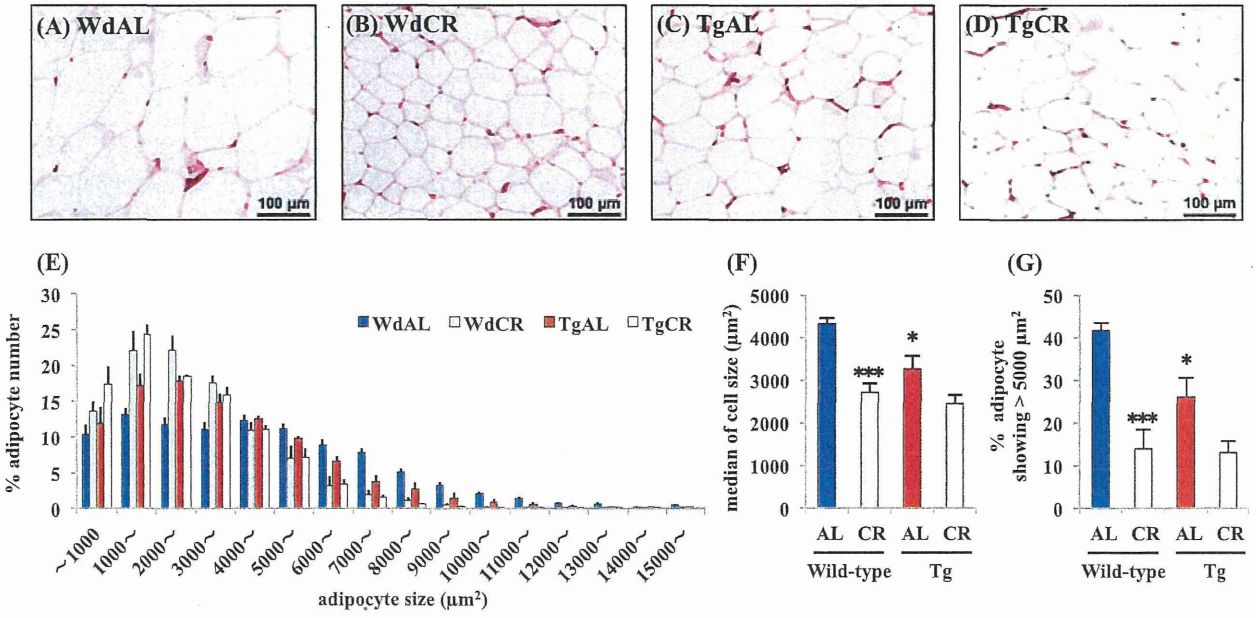

Fig. 1 Effects of CR and Tg on morphologic features of white adipose tissue. Representative hematoxylin/eosin-stained histological sections of WAT from WdAL (**a**), WdCR (**b**), TgAL (**c**), and TgCR (**d**) rats (magnification ×40; *scale bar* 100 μm). **e** Distribution of adipocyte sizes in wild-type and tg rats. **f** Median of adipocyte sizes in wild-type and Tg rats. **g** The percentage of adipocytes showing >5,000 μm^2 in wild-type and Tg rats. Adipocyte size was calculated based on a quantitative morphometric method using ImageJ 1.43u/Java1.6.0_22 software. *Error bars* are SEM for each group (n=4). Approximately 1,000–2,100 adipocytes were counted per rat. *P<0.05 and ***P< 0.001 vs. WdAL (Tukey's t test)

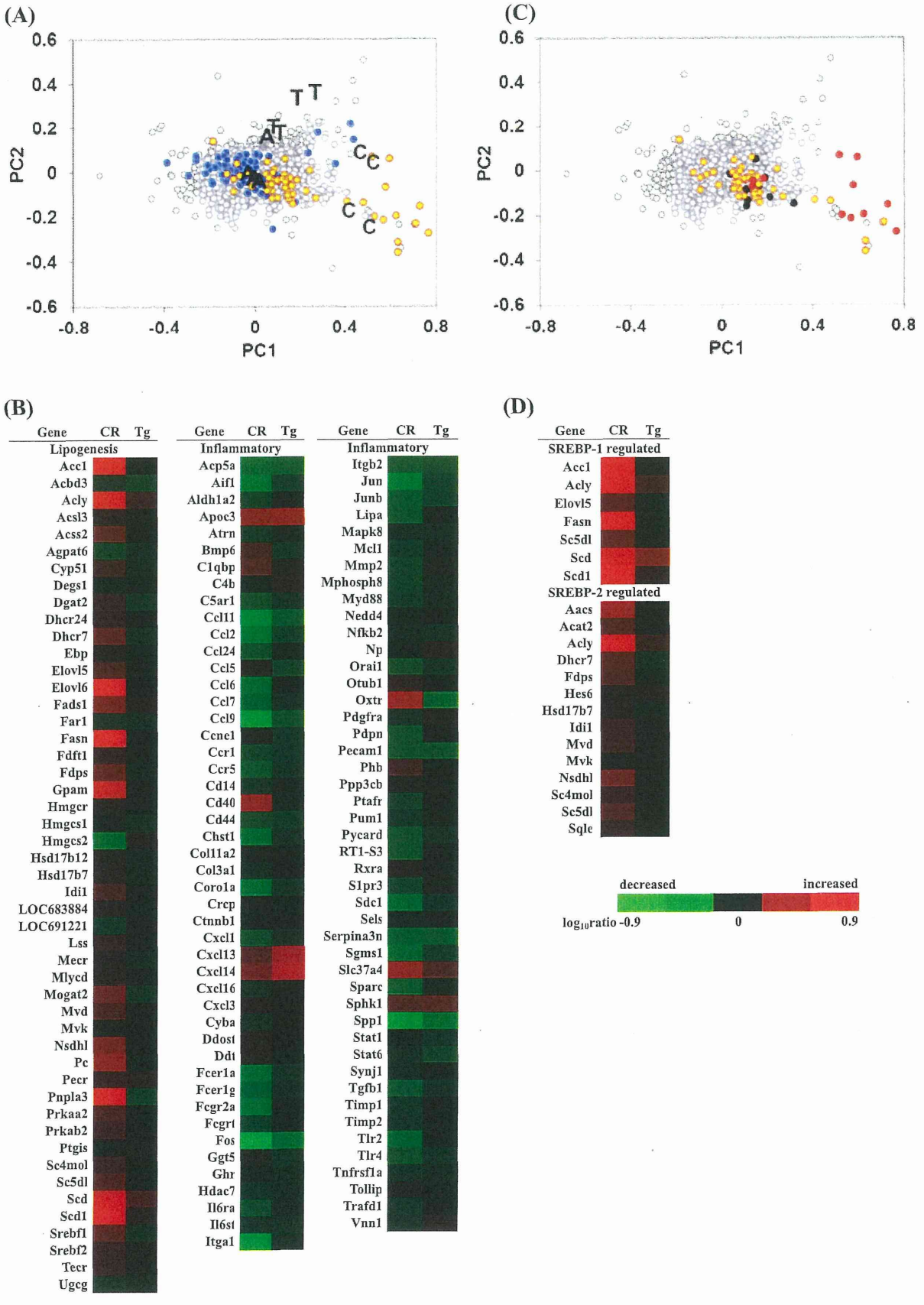
(A)
PC2
PC1
T T
A T
C C
C C
(C)
PC2
PC1
(B)
Gene CR Tg
Lipogenesis
Acc1
Acbd3
Acly
Acsl3
Acss2
Agpat6
Cyp51
Degs1
Dgat2
Dhcr24
Dhcr7
Ebp
Elovl5
Elovl6
Fads1
Far1
Fasn
Fdft1
Fdps
Gpam
Hmgcr
Hmgcs1
Hmgcs2
Hsd17b12
Hsd17b7
Idi1
LOC683884
LOC691221
Lss
Mecr
Mlycd
Mogat2
Mvd
Mvk
Nsdhl
Pc
Pecr
Pnpla3
Prkaa2
Prkab2
Ptgis
Sc4mol
Sc5dl
Scd
Scd1
Srebf1
Srebf2
Tecr
Ugcg
Gene CR Tg
Inflammatory
Acp5a
Aif1
Aldh1a2
Apoc3
Atrn
Bmp6
C1qbp
C4b
C5ar1
Ccl11
Ccl2
Ccl24
Ccl5
Ccl6
Ccl7
Ccl9
Ccne1
Ccr1
Ccr5
Cd14
Cd40
Cd44
Chst1
Col11a2
Col3a1
Coro1a
Crcp
Ctnnb1
Cxcl1
Cxcl13
Cxcl14
Cxcl16
Cxcl3
Cyba
Ddost
Ddt
Fcer1a
Fcer1g
Fcgr2a
Fcgrt
Fos
Ggt5
Ghr
Hdac7
Il6ra
Il6st
Itga1
Gene CR Tg
Inflammatory
Itgb2
Jun
Junb
Lipa
Mapk8
Mcl1
Mmp2
Mphosph8
Myd88
Nedd4
Nfkb2
Np
Orai1
Otub1
Oxtr
Pdgfra
Pdpn
Pecam1
Phb
Ppp3cb
Ptafr
Pum1
Pycard
RT1-S3
Rxra
S1pr3
Sdc1
Sels
Serpina3n
Sgms1
Slc37a4
Sparc
Sphk1
Spp1
Stat1
Stat6
Synj1
Tgfb1
Timp1
Timp2
Tlr2
Tlr4
Tnfrsf1a
Tollip
Trafd1
Vnn1
(D)
Gene CR Tg
SREBP-1 regulated
Acc1
Acly
Elovl5
Fasn
Sc5dl
Scd
Scd1
SREBP-2 regulated
Aacs
Acat2
Acly
Dhcr7
Fdps
Hes6
Hsd17b7
Idi1
Mvd
Mvk
Nsdhl
Sc4mol
Sc5dl
Sqle
decreased
increased
log10ratio -0.9
0
0.9

to compare the frequencies of genes matching specific categories or keywords in the GO Biological Process database; genes with $P<0.001$ are presented in Table 2. Among the 199 genes with PC1 >0.16, several were involved in metabolic processes, particularly lipid biosynthesis (GO 0008610, 0006633, and 0019432). Among the 226 genes with PC1 < –0.16, several genes were related to inflammation (GO 0006955, 0006954, 0034097, and 0030593).

To better define the effects of CR and Tg, the selected genes are indicated with yellow dots (GO 0008610, 0006633, and 0019432) and blue dots (GO 0006955, 0006954, 0034097, and 0030593) in the scatter plot (Fig. 2a), and are shown in a heat map (Fig. 2b). CR enhanced the expression of several genes involved in lipid biosynthesis (GO 0008610, 0006633, and 0019432) and suppressed the expression of genes involved in inflammation (GO 0006955, 0006954, 0034097, and 0030593). In contrast, Tg did not affect the expression of most of these genes. The effects of Tg appeared in PC2 as the groups located next to the axis; however, very few genes had large scores (Fig. 2a). In fact, we found no biological processes that were only affected by Tg (Table 2).

SREBPs are master transcriptional regulators of lipid metabolism and adipocyte differentiation. Three SREBP isoforms, 1a, 1c, and 2 have been identified (Osborne 2000; Osborne and Espenshade 2009). All three isoforms are synthesized as long inactive precursors, and SREBP cleavage-activating protein (SCAP) is required to convert these inactive precursors to transcriptionally active forms (Osborne 2000; Osborne and Espenshade 2009). Horton et al. identified and listed the genes regulated by SREBP-1 and SREBP-2 in vivo using transcriptome analysis of the liver of SREBP-1a transgenic, SREBP-2 transgenic, and SCAP knockout mice (Horton et al. 2003). We compared our data with theirs, and the SREBP-1- and SREBP-2-regulated genes are shown in a scatter plot with red and black dots, respectively (Fig. 2c). The SREBP-1- and SREBP-2-regulated genes identified by Horton et al. were observed in our heat map (Fig. 2d). SREBP-1-regulated genes were exclusively upregulated by CR, whereas SREBP-2-regulated genes were not, except for *ATP-citrate lyase* (*Acly*), which was also upregulated by SREBP-1 (Fig. 2c and d). Next, we examined the expression levels of *SREBP-1a*, *1c*, and *2*, and the genes regulated by SREBP-1 and SREBP-2 using real-time RT-PCR. We found that the expression of *SREBP*s was increased in WdCR, but not in TgAL, compared with WdAL. Among the *SREBP*s, it appears that CR had the strongest effect on *SREBP-1c* expression, followed by *SREBP-1a*, and the weakest effect on *SREBP-2* expression (Fig. 3a). The SREBP-1-regulated genes, *FASN* and *ACC1*, were upregulated in WdCR, but not in TgAL (Fig. 3b). In contrast, the SREBP-2-regulated genes, *Sqle* and *Mvk*, were not significantly upregulated in either WdCR or TgAL (Fig. 3c).

It is well-known that macrophages play a key role in inflammation in WAT of obese animals (Ouchi et al. 2011). An increased expression of MCP-1 [also known as chemokine (C-C motif) ligand 2] in WAT contributes to macrophage infiltration into WAT in obese mice (Kanda et al. 2006). Moreover, obesity leads to a shift from M2 (alternatively activated) macrophages to M1 (classically activated) macrophages in WAT (Lumeng et al. 2007). Therefore, we examined the expression of genes encoding the macrophage-specific transmembrane proteins, *F4/80*, *MCP-1*, the M1 macrophage-specific marker *CD11c* (also known as *integrin alpha X*), and the M2 macrophage-specific marker *CD163* (Kawanishi et al. 2010). As expected, the expression of *F4/80*, *MCP-1*, and *CD11c* was downregulated in WdCR, but not in TgAL, compared with WdAL. In contrast, CR and Tg did not significantly affect the expression of *CD163* (Fig. 3d).

◀ **Fig. 2** Principal component analysis of gene expression. **a** PC ordination of 6,641 ANOVA-positive genes based on the DNA microarray data of WdAL, WdCR, and TgAL (four biological repeats per group). *A*, *C*, and *T* represent WdAL, WdCR, and TgAL rats, respectively. The *yellow and blue dots* represent genes involved in lipid biosynthesis and inflammation, respectively. Gene function was defined based on annotations in the Gene Ontology (GO) Biological Process database (release 31) provided by the manufacturer. Genes involved in lipid biosynthesis were derived from the gene lists (GO: 0008610, 0006633, and 0019432). Genes involved in inflammation were derived from the gene lists (GO: 0006955, 0006954, 0034097, and 0030593). **b** Heat map of genes involved in lipid biosynthesis and inflammation. Genes involved in lipid biosynthesis were mostly upregulated by CR, while those involved in inflammation were predominantly downregulated by CR. The expression of these genes was not influenced by Tg. **c** Scatter plots of SREBP-1- (*red*) and SREBP-2- (*black*) regulated genes listed by Horton et al. (2003). All of the genes were included in the genes listed in GO 0008610, 0006633, and 0019432 (*yellow*). **d** Heat map of SREBP-1- and SREBP-2-regulated genes identified by Horton et al. (2003). Most of the SREBP-1-regulated genes were upregulated by CR, while most of the SREBP-2-regulated genes were not affected by CR

Table 2 List of ratios and *P* values of the selected GO terms

Gene ontology PC1>0	Biological process 199 genes selected	Ratio	*P* values
0008152	Metabolic process	37/756	7.9E-15
0055114	Oxidation reduction	23/591	8.2E-12
0008610	Lipid biosynthetic process	16/92	5.0E-14
0006629	Lipid metabolic process	13/232	5.2E-09
0006633	Fatty acid biosynthetic process	12/59	1.2E-14
0005975	Carbohydrate metabolic process	10/206	1.1E-06
0014070	Response to organic cyclic substance	9/274	8.1E-05
0008283	Cell proliferation	8/190	3.7E-05
0050873	Brown fat cell differentiation	7/34	3.5E-09
0006096	Glycolysis	7/45	2.3E-08
0016477	Cell migration	7/112	9.6E-06
0045471	Response to ethanol	7/153	6.8E-05
0010033	Response to organic substance	7/163	1.0E-04
0006090	Pyruvate metabolic process	6/21	6.9E-09
0009749	Response to glucose stimulus	6/118	1.3E-04
0006084	Acetyl-CoA metabolic process	5/11	1.3E-08
0019432	Triglyceride biosynthetic process	5/13	3.0E-08
0006641	Triglyceride metabolic process	5/40	7.1E-06
0005977	Glycogen metabolic process	5/42	9.0E-06
0006086	Acetyl-CoA biosynthetic process from pyruvate	4/7	1.6E-07
0009267	Cellular response to starvation	4/23	1.7E-05
0016126	Sterol biosynthetic process	4/28	3.6E-05
0006695	Cholesterol biosynthetic process	4/32	6.1E-05
0033574	Response to testosterone stimulus	4/41	1.6E-04
0009058	Biosynthetic process	4/58	5.8E-04
0042593	Glucose homeostasis	4/62	7.4E-04
0007595	Lactation	4/65	8.8E-04
PC1<0	226 genes selected		
0006955	Immune response	10/243	1.5E-05
0043066	Negative regulation of apoptosis	9/284	2.7E-04
0006954	Inflammatory response	7/170	2.8E-04
0030509	BMP signaling pathway	6/65	9.8E-06
0034097	Response to cytokine stimulus	6/119	2.7E-04
0030900	Forebrain development	5/94	6.9E-04
0009612	Response to mechanical stimulus	5/102	9.9E-04
0016525	Negative regulation of angiogenesis	4/29	6.8E-05
0030593	Neutrophil chemotaxis	4/35	1.4E-04
PC2>0	65 genes selected		
No annotation was significantly marked			
PC2<0	118 genes selected		
0051384	Response to glucocorticoid stimulus	5/163	4.3E-04
0048545	Response to steroid hormone stimulus	4/64	1.1E-04
0006006	Glucose metabolic process	4/79	2.6E-04

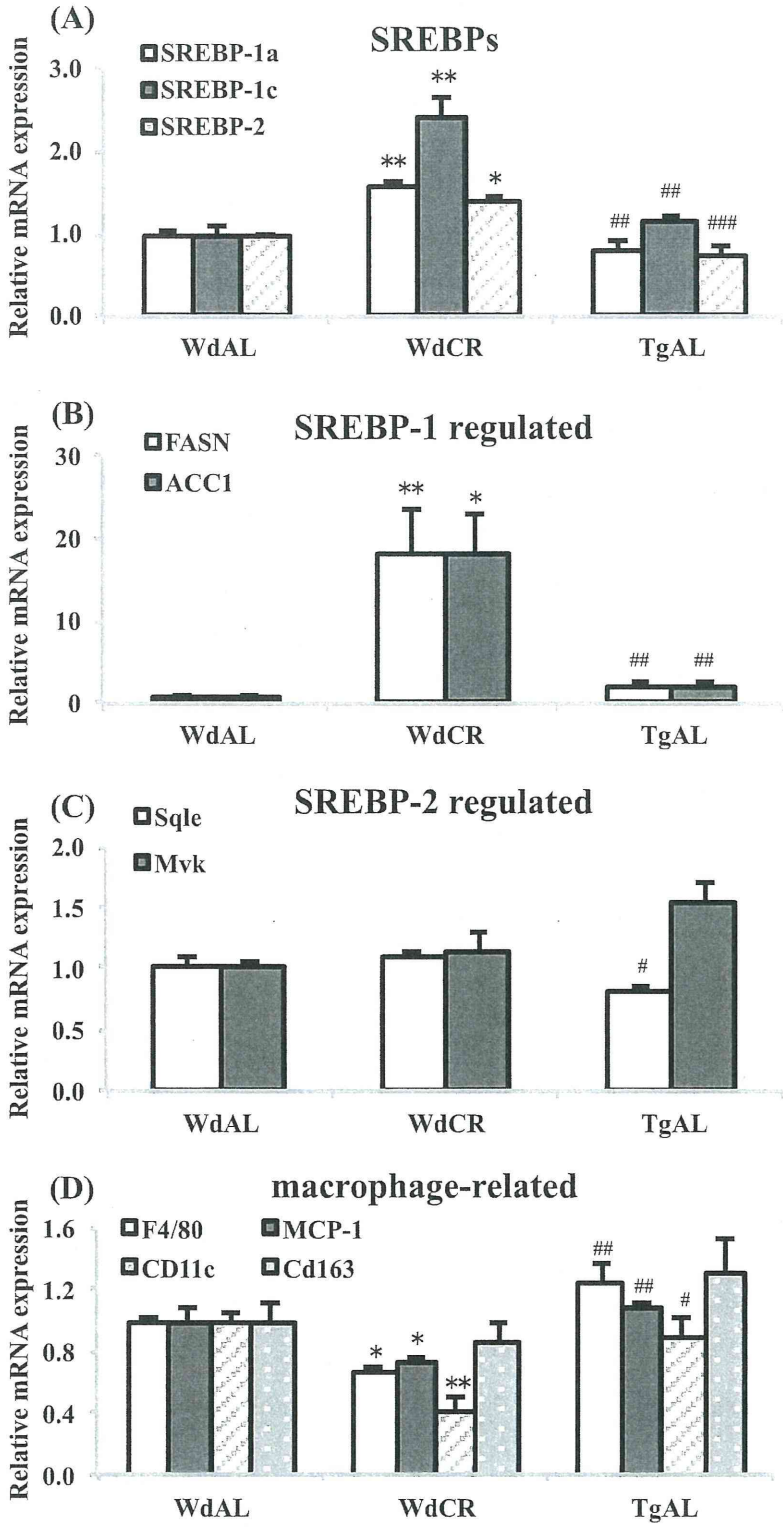

Fig. 3 Quantitative analysis of the mRNA expression of *SREBP*s, SREBP-1-regulated genes, SREBP-2-regulated genes, and macrophage-related genes in WdAL, WdCR, and TgAL rats. The mRNA expression levels in WAT of *SREBP*s (*A*: *SREBP-1a*, *SREBP-1c*, and *SREBP-2*), SREBP-1-regulated genes [*B*: *fatty acid synthase* (*FASN*) and *acyl CoA carboxylase 1* (*ACC1*)], SREBP-2-regulated genes [*C*: *squalene epoxidase* (*Sqle*) and *mevalonate kinase* (*Mvk*)], and macrophage-related genes [*D monocyte chemotactic protein-1* (*MCP-1*), *F4/80*, *integrin alpha X* (*Itgax*, *CD11c*), and *CD163*] were analyzed by real-time RT-PCR. Data were normalized against *TBP* expression. Values are means±SEM (n=3–6). *P<0.05, **P<0.01, and ***P<0.001 vs. WdAL; $^{\#}P$<0.05, $^{\#\#}P$<0.01, and $^{\#\#\#}P$<0.001 vs. WdCR (Tukey's t test)

To confirm the CR-associated SREBP-1- and macrophage-related gene expression profiles observed in wild-type rats, we analyzed the effect of CR on Tg rats. Similarly to the wild-type rats, CR markedly upregulated the expression of *SREBP-1c*, and slightly increased the expression of *SREBP-1a* (P=0.08; Fig. 4a). CR also markedly enhanced the expression of the SREBP-1-regulated genes, *FASN* and *ACC1*

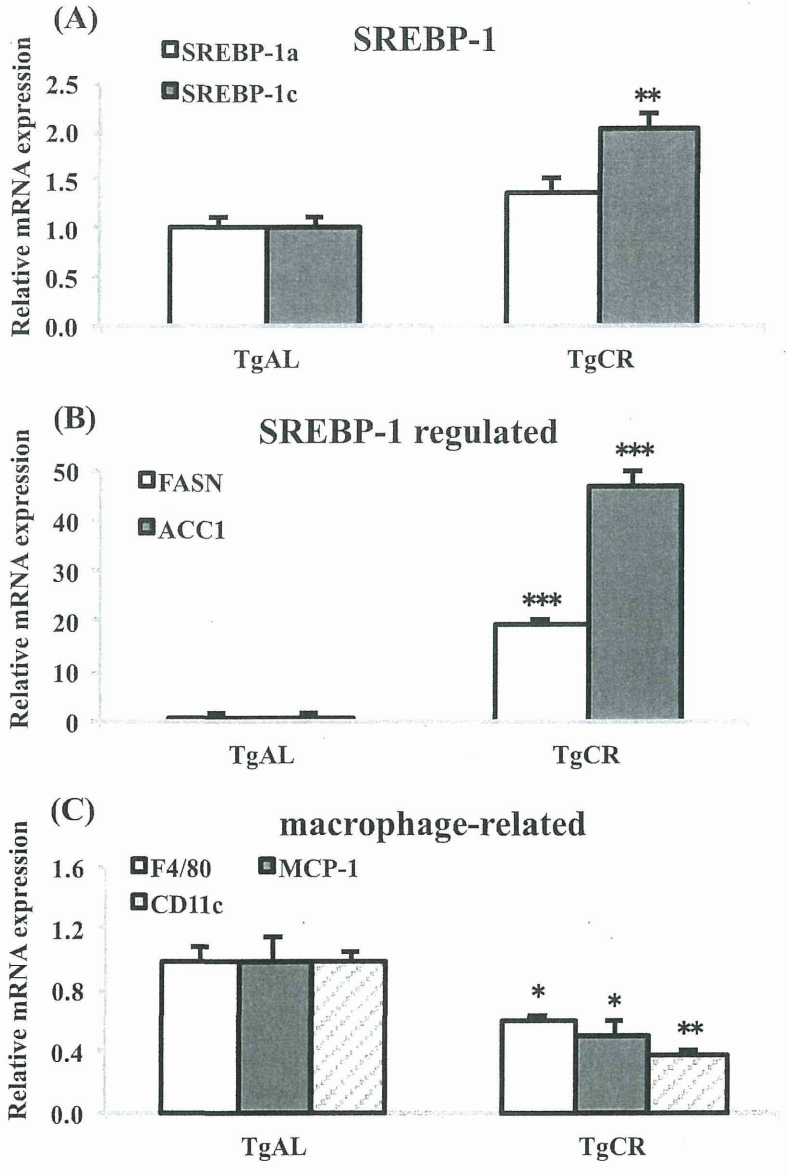

Fig. 4 Quantitative analysis of the mRNA expression of *SREBP*s, SREBP-1-regulated genes, and macrophage-related genes in TgAL and TgCR rats. The mRNA expression levels in WAT of *SREBP*s (**a** *SREBP-1a* and *SREBP-1c*), SREBP-1-regulated genes [**b** *fatty acid synthase* (*FASN*) and *acyl CoA carboxylase 1* (*ACC1*)], and macrophage-related genes [**c** *F4/80*, *monocyte chemotactic protein-1* (*MCP-1*), *integrin alpha X* (*Itgax*, *CD11c*)] were analyzed by real-time RT-PCR. Data were normalized against *TBP* expression. Values are means±SEM (n=4–5). *P<0.05, **P<0.01, and ***P<0.001 vs. TgAL (Tukey's t test)

(Fig. 4b), while it significantly downregulated the expression of the macrophage-involved genes, *F4/80*, *MCP-1*, and *CD11c* in Tg rats (Fig. 4c).

Discussion

In the current study, we found that CR markedly reduced the size of adipocytes in WAT of wild-type rats (Fig. 1a, b, f, and g), but this CR effect was blunted in Tg rats (Fig. 1c, d, f, and g). Tg also significantly reduced adipocyte size, but this effect of Tg was less than that of CR (Fig. 1a, b, c, f, and g). When looking at adiposity (WAT weight as a percentage of body weight), the effect of CR was predominantly found in wild-type rats rather than Tg rats. It is well-known that small adipocytes secrete more adiponectin and less pro-inflammatory cytokines, including TNF-α and leptin, and are generally more sensitive to insulin (Ouchi et al. 2011). Moreover, small adipocytes act as powerful buffers by absorbing lipids in the postprandial period. If this buffering action is impaired, lipids in the form of TG accumulate in non-adipose tissues, resulting in insulin resistance (Frayn 2002). Recently, it has been reported that inflammatory cells preferentially infiltrate into WAT containing large adipocytes (Ouchi et al. 2011). Therefore, the CR-associated adipokine profile, the